

# Coupling of Baryon Resonances to the $N\omega$ channel<sup>\*</sup>

M. Post and U. Mosel

*Institut für Theoretische Physik, Universität Giessen,  
D-35392 Giessen, Germany*

*and*

*Nuclear Science Division, Lawrence Berkeley National Laboratory  
Berkeley, CA 94720, USA*

## Abstract

We estimate the resonance coupling strength  $f_{RN\omega}$  and  $f_{RN\rho}$  from a Vector Meson Dominance (VMD) analysis. The isoscalar and isovector part of the photon coupling are obtained separately from helicity amplitudes. The reliability of this approach is tested by comparing VMD predictions for  $f_{RN\rho}$  with values obtained from fitting the hadronic decay widths into  $N\rho$ . A reasonable agreement is found, but VMD tends to underestimate the coupling constants. In order to confirm consistency with experimental data, we calculate the cross-sections for photon-and pion induced reactions within a *Breit-Wigner* model. Finally, we study how the properties of  $\omega$  mesons in nuclear matter are affected from the excitation of resonance-hole loops. For an  $\omega$  at rest, we find a broadening of about 40 MeV, while at higher momenta the effect of resonance excitations is reduced.

PACS: 12.40.Vv, 13.40.Hq, 13.60.-r, 14.40.Cs, 13.60.-r, 21.65.+f

Keywords: Resonance Decay, Vector Meson Dominance, Breit-Wigner Model, Nuclear Matter, Omega Spectral Function

---

<sup>\*</sup>Work supported by BMBF and DFG.

# 1 Introduction

Up to now a satisfactory understanding of baryon resonances in the  $N\omega$  channel has not been achieved. A number of experiments on the photoproduction of  $\omega$  mesons have displayed indications for resonant structures [1]. However the data basis is not sufficiently broad to allow for an unique determination of the quantum numbers of the involved resonances. Thus – based mostly on quark models – a number of resonances in the mass range of approximately 1.8 – 2 GeV have been proposed to show a sizeable coupling to the  $\omega$  meson [2, 3, 4]. On the other hand, no experimental evidence for the existence of baryon resonances in the  $N\omega$  system has been reported from the reaction  $\pi N \rightarrow \omega N$  [5].

An understanding of baryon resonances in the  $N\omega$  channel is not only important for a description of scattering experiments, but might also be of interest as far as the properties of  $\omega$  mesons in nuclear matter are concerned. This conjecture is guided from the experience with the  $\rho$  meson, which has been shown to undergo significant modification in the nuclear medium due to the excitation of resonance-hole loops. In this scenario a central role is played by the subthreshold resonance  $D_{13}(1520)$  [6, 7, 8], suggesting that especially information on the coupling strength of subthreshold resonances to the  $N\omega$  system would be very valuable for a determination of the in-medium properties of the  $\omega$  meson.

In this work we present estimates for the coupling strength of baryon resonances to the  $\omega N$  channel  $f_{RN\omega}$ . Vector Meson Dominance (VMD) is utilized to relate  $f_{RN\omega}$  to the isoscalar strength of the electromagnetic decay of the respective resonance, which is extracted from helicity amplitudes. The analysis covers all resonances for which helicity amplitudes are currently available [9, 10], most of which are below the nominal  $\omega N$  threshold. A coupling of subthreshold resonances to the  $N\omega$  system has also been reported elsewhere [8, 11]. In [8] such a mechanism is found to be necessary for a satisfactory description of  $\pi N$  scattering within a coupled-channel analysis, whereas the authors of [11] derive the coupling strength within a quark-model approach. We will compare our results with those of both works.

The paper is organized as follows. The details of the extraction of  $f_{RN\omega}$  are presented in Sect. 2. In Sect. 3 we examine if our model gives reasonable results by comparing the VMD prediction for the isovector strength with fits to the hadronic decay width into the  $N\rho$  channel. Sect. 4 is devoted to a presentation of the results for  $f_{RN\omega}$  and a discussion of their compatibility

with experimental information on the reactions  $\pi N \rightarrow \omega N$  and  $\gamma N \rightarrow \omega N$ . Finally, in Sect. 5 the implications of excitations of resonance-hole loops for the in-medium properties of  $\omega$  mesons are examined.

## 2 Determination of $f_{RN\omega}$

In this section we explain how we obtain an estimate for the magnitude of the coupling strength of a baryonic resonance to the  $N\omega$  channel. Before going into the details of the calculation, we outline the basic idea of our approach.

Vector Meson Dominance (VMD) [12], a theory which describes photon-hadron interactions exclusively in terms of vector meson-hadron interactions, relates the hadronic coupling strength of resonances to vector mesons  $f_{RN\rho(\omega)}$  and the isoscalar and isovector part of the photon-coupling, see Fig. 1:

$$\begin{aligned} f_{RN\omega} &= g_s m_\omega \frac{2 g_\omega}{e} \\ f_{RN\rho} &= g_v m_\rho \frac{2 g_\rho}{e} . \end{aligned} \tag{1}$$

As values for  $g_\rho$  and  $g_\omega$  – the coupling strengths of  $\rho$  and  $\omega$  meson to the photon – we take  $g_\rho = 2.5$  and  $g_\omega = 8.7$  [12]. The isoscalar and isovector coupling strength of the resonance to the  $N\gamma$  system is given by  $g_s$  and  $g_v$ , respectively, see Eq. 3.

Thus VMD gives access to both  $f_{RN\omega}$  and  $f_{RN\rho}$ , if it is possible to obtain  $g_s$  and  $g_v$  from experimental data. In order to achieve this goal, it is clearly not sufficient to consider merely the total electromagnetic decay width of the resonance. Rather, the coupling has to be decomposed into an isoscalar and an isovector part, which is readily done by constructing suitable linear combinations of proton- and neutron-amplitudes. These amplitudes are known from experiment [9, 10], thus allowing to deduce numerical values for  $g_s$  and  $g_v$ .

In a nonrelativistic formulation, the coupling of baryon resonances to the photon-nucleon system can be formulated as [6, 13]:

$$\mathcal{L}_{RN\gamma} = \begin{cases} \chi_R^\dagger \epsilon_{ijk} \sigma^i q^j \epsilon_\lambda^k \chi_N I + h.c. & \text{for } J^P = \frac{1}{2}^+ \\ \chi_R^\dagger \epsilon_{ijk} S^i q^j \epsilon_\lambda^k \chi_N I + h.c. & \text{for } J^P = \frac{3}{2}^+ \\ \chi_R^\dagger R_{ij} F_\lambda^{ij} \chi_N I + h.c. & \text{for } J^P = \frac{5}{2}^+ \\ \chi_R^\dagger (\sigma_k \epsilon_\lambda^k \omega - \sigma_k q^k \epsilon_\lambda^0) \chi_N I + h.c. & \text{for } J^P = \frac{1}{2}^- \\ \chi_R^\dagger (S_k \epsilon_\lambda^k \omega - S_k q^k \epsilon_\lambda^0) \chi_N I + h.c. & \text{for } J^P = \frac{3}{2}^- \end{cases} \quad (2)$$

Here  $\chi_R^\dagger$  and  $\chi_N$  denote resonance and nucleon spinors respectively. The  $\sigma^i$  are the Pauli matrices,  $S^i$  denotes the spin- $\frac{3}{2}$  and  $R^{ij}$  the spin- $\frac{5}{2}$  transition operator.  $q$  is the c.m. momentum of the photon,  $\omega$  its energy and  $\epsilon_\lambda$  its polarization vector.  $F_\lambda^{ij}$  denotes the spatial components of the electromagnetic field strength tensor  $F_\lambda^{\mu\nu}$  with  $F_\lambda^{ij} = q^i \epsilon_\lambda^j - q^j \epsilon_\lambda^i$ . By  $I$  we denote the isospin part of the coupling which is given as:

$$I = \chi_R^{I\dagger} \left( g_s + g_v \begin{Bmatrix} \sigma^3 \\ S^3 \end{Bmatrix} \right) \chi_N^I \quad \text{for} \quad \begin{cases} I_R = \frac{1}{2} \\ I_R = \frac{3}{2} \end{cases} \quad (3)$$

The spinors  $\chi_R^I$  and  $\chi_N^I$  represent resonance and nucleon isospinors and  $I_R$  denotes the isopin of the resonance.  $\sigma^3$  and  $S^3$  are defined as above.

Note that the invariant amplitude – as derived from (2) and (3) – for the decay of a resonance into a proton,  $\mathcal{M}_p$ , is proportional to  $g_p = g_s + \alpha g_v$ , whereas for the neutron the amplitude  $\mathcal{M}_n$  is proportional to  $g_n = g_s - \alpha g_v$ . The factor  $\alpha$  is defined as:

$$\alpha = \chi_R^{I\dagger} \begin{Bmatrix} \sigma^3 \\ S^3 \end{Bmatrix} \chi_N^I \quad (4)$$

For nucleon resonances it is 1 and for  $\Delta$  resonances it is exactly the Clebsch-Gordan coefficient for the respective transition, in this case  $\alpha = \sqrt{\frac{2}{3}}$  [14].

Thus, the linear combinations

$$\mathcal{M}_s = \frac{1}{2} (\mathcal{M}_p + \mathcal{M}_n) \quad (5)$$

$$\mathcal{M}_v = \frac{1}{2} (\mathcal{M}_p - \mathcal{M}_n) \begin{cases} 1 & \text{for } I_R = \frac{1}{2} \\ \frac{1}{\alpha} & \text{for } I_R = \frac{3}{2} \end{cases}$$

are proportional to  $g_s$  and  $g_v$  respectively.  $\mathcal{M}_s$  and  $\mathcal{M}_v$  describe the  $RN\gamma$  system in terms of the isospin of the photon rather than the isospin of the nucleon.

Experimental information on the decay amplitudes  $\mathcal{M}_p$  and  $\mathcal{M}_n$  exists in form of measured helicity amplitudes  $A_{\frac{1}{2}}^{p/n}$  and  $A_{\frac{3}{2}}^{p/n}$ . They describe the transition of the photon-proton and the photon-neutron system to a resonance state with  $j_z = \frac{1}{2}$  or  $\frac{3}{2}$ , where the quantization axis is defined along the direction of the photon momentum. From the helicity amplitudes the isoscalar and isovector part of the coupling are constructed in exactly the same way as shown in Eq. 5 for the Feynman amplitudes. The helicity amplitudes are known from experiment at the pole-mass of the resonance, allowing the determination of  $g_s$  and  $g_v$ .

To this end we introduce the  $\gamma$ -width  $\Gamma_{s/v}^\gamma$ , which – using the normalization from [10] – is defined in terms of the helicity amplitudes  $A_{s/v}$  in the following way:

$$\Gamma_{s/v}^\gamma(m_R) = \frac{q^2}{\pi} \frac{2m_N}{(2j_R + 1)m_R} \left( |A_{\frac{1}{2}}^{s/v}|^2 + |A_{\frac{3}{2}}^{s/v}|^2 \right) \quad , \quad (6)$$

with  $j_R$  and  $m_R$  denoting spin and pole-mass of the resonance. Note that after the angular integration has been performed no interference terms between  $A_{\frac{1}{2}}^{s/v}$  and  $A_{\frac{3}{2}}^{s/v}$  appears in Eq. 6.

Clearly,  $\Gamma_{s/v}^\gamma$  can also be expressed using Feynman amplitudes:

$$\Gamma_{s/v}^\gamma(k^2) = \frac{1}{(2j_R + 1)} \frac{q}{8\pi k^2} |\mathcal{M}_{s/v}|^2 \quad , \quad (7)$$

where  $\sqrt{k^2}$  is the invariant mass of the resonance and  $q$  the momentum of the photon in the rest frame of the resonance. After summing over the photon polarizations,  $|\mathcal{M}_s|^2$  assumes the following form:

$$|\mathcal{M}_s|^2 = 4 m_N m_R \kappa g_s^2 q^2 F(k^2) \quad . \quad (8)$$

The same relation holds for  $|\mathcal{M}_v|^2$  with  $g_s$  replaced by  $g_v$ . For the formfactor  $F(k^2)$  at the  $RN\gamma$  vertex we assume the following functional dependence

[7, 15, 16]:

$$F(k^2) = \frac{\Lambda^4}{\Lambda^4 + (k^2 - m_R^2)^2} \quad (9)$$

with  $\Lambda = 1$ . If we consider on-resonance decays ( $\sqrt{k^2} = m_R$ ) this formfactor is equal to 1. The numerical factor  $\kappa$  depends on the quantum numbers of the resonance. For isospin- $\frac{1}{2}$  resonances the values for  $\kappa$  are listed in Table 2. In the case of  $\Delta$  resonances they need to be multiplied by a factor of  $F^2 = \frac{2}{3}$  due to isospin. The two expressions Eqs. 6 and 7 can now be equated allowing to solve for  $g_{s/v}$ :

$$g_{s/v}^2 = \frac{4}{\kappa} \frac{|A_{\frac{1}{2}}^{s/v}|^2 + |A_{\frac{3}{2}}^{s/v}|^2}{q} \begin{cases} 1 & \text{for } I_R = \frac{1}{2} \\ \frac{1}{F^2} & \text{for } I_R = \frac{3}{2} \end{cases} . \quad (10)$$

Again, in the case of  $\Delta$  resonances an additional factor  $\alpha^2$  needs to be introduced.

Thus it is possible to obtain  $g_{s/v}$  from helicity amplitudes. The hadronic couplings  $f_{RN\omega(\rho)}$  are then readily deduced from the VMD relation Eq. 1. The corresponding values are listed in Tables 1 and 2.

A modified version of VMD (called VMD1 in [12]) contains also a direct coupling between hadrons – in our case baryon resonances – and the photon. In particular, at the photon point  $q^2 = 0$  the photon-resonance interaction proceeds without intermediate vector mesons, whereas the decay into a massive photon consists of both a direct coupling term and a term with an intermediate vector meson. In principle, it would be preferable to perform an analysis such as ours within the framework of the modified version of VMD by studying – currently unavailable – dilepton production data on the nucleon. This process involves massive photons and would, in combination with the data for real photons, allow one to disentangle the direct photon and vector meson contribution. As a further advantage, the coupling strength of the vector mesons then does not need to be extrapolated over the large mass range from the photon point to the on-shell mass of  $\rho$  and  $\omega$  meson.

### 3 Results for the $\rho$ : How Reliable is VMD ?

In this section we study the applicability of VMD in the resonance region. This is done for the isovector part of the analysis, where the VMD predictions

for  $f_{RN\rho}$  can be compared with the measured resonance decay width into the  $N\rho$  channel.

We consider all resonances with  $j_R < \frac{7}{2}$ , for which both the hadronic decay widths into  $N\rho$  and the helicity amplitudes are known. This excludes a few light resonances like the  $S_{11}(1535)$  and the  $P_{33}(1600)$ , for which only upper limits for the  $N\rho$  branching ratio exist [10]. For both the helicity amplitudes and for the partial  $N\rho$  decay width we use different parameter sets in order to provide an estimate for the experimental uncertainties entering this analysis. The helicity amplitudes are taken from Arndt *et al* [9] and the PDG [10]. Furthermore we use the values obtained in the work of [15], which is of particular interest as it represents the only available approach which describes simultaneously hadronic-and electromagnetic reactions over the full energy region of interest here. The  $\rho$  decay widths are taken from the analysis of Manley *et al* [18, 19] and the PDG [10]. Furthermore, we study the additional model dependence introduced by different parameterizations of the spectral function of the  $\rho$  meson.

The hadronic coupling constant  $f_{RN\rho}$  is obtained via the following expression for the  $R \rightarrow N\rho$  decay width (taken on the pole mass of the resonance)[6]:

$$\Gamma_{R \rightarrow N\rho} = \frac{1}{8\pi m_R^2} \frac{1}{2j_R + 1} \int_{2m_\pi}^{m_R - m_N} dm \, 2m \, A_\rho(m) |\mathcal{M}_{R \rightarrow N\rho}|^2 \mathbf{q} \quad . \quad (11)$$

The decay amplitude  $\mathcal{M}_{R \rightarrow N\rho}$  is obtained from the same Lagrangians as in the electromagnetic case and is proportional to  $f_{RN\rho}$  [6].  $\mathbf{q}$  is the three momentum of the  $\rho$  meson in the rest frame of the resonance. Note that there is no formfactor in Eq. 11 because we consider the on-resonance decay.

The spectral function of the  $\rho$  meson  $A_\rho(m)$  is taken as:

$$A_\rho(m) = \frac{1}{\pi} \frac{m \Gamma(m)}{(m^2 - m_\rho^2)^2 + m^2 \Gamma^2(m)} \quad . \quad (12)$$

The decay into  $N\rho$  of low-lying resonances, for example the  $D_{13}(1520)$ , proceeds mainly through the low-mass tail of  $A_\rho$ . The shape of the tail is quite sensitive to the parameterization of the  $\rho$  decay width. To study the effect on  $f_{RN\rho}$  we compare two different parameterizations of the  $\rho$  decay width:

$$\Gamma(m) = \left( \frac{m_\rho}{m} \right)^2 \Gamma_0 \left( \frac{\mathbf{p}_m}{\mathbf{p}_{m_\rho}} \right)^3 \quad (13)$$

and

$$\Gamma(m) = \left(\frac{m_\rho}{m}\right) \Gamma_0 \left(\frac{\mathbf{p}_m}{\mathbf{p}_{m_\rho}}\right)^3 \frac{1 + r^2 \mathbf{p}_{m_\rho}^2}{1 + r^2 \mathbf{p}_m^2} . \quad (14)$$

The first version follows from a one-loop approximation of the self energy of the  $\rho$  meson [6, 17], the second one is taken from the PDG [10].  $m$  is the invariant mass of the  $\rho$  meson,  $m_\rho = 0.768$  GeV its pole mass and  $\Gamma_0 = 150$  MeV its decay width on the pole mass.  $\mathbf{p}_{m_\rho}(\mathbf{p}_m)$  denotes the 3-momentum of the pions measured in the rest frame of a decaying  $\rho$  meson with mass  $m_\rho(m)$ . The range parameter  $r$ , appearing in the second expression has the numerical value  $r = 5.3/\text{GeV}$  [10].

In Table 1 the results for the coupling constants and the corresponding error-bars - which are calculated from the error-bars assigned to the partial decay width and the helicity amplitude in the respective analysis - are given. As a general tendency, our finding is that VMD works well within a factor of two. It tends to somewhat underestimate the coupling constants, leaving some room for an additional direct coupling of the resonance to the photon. This can be seen particularly well in the case of the  $D_{13}(1520)$  and the  $F_{15}(1680)$ , which are the most prominent resonances in photon-nucleon reactions, and whose  $\rho$  decay widths are also well under control. Note that in the case of the  $S_{31}(1620)$  and the  $P_{13}(1720)$  large discrepancies occur between the VMD predictions based on different sets of helicity amplitudes, thus reflecting the uncertainties inherent in this analysis. The helicity amplitudes from Arndt [9] and PDG [10] produce nearly identical results for the  $\rho$  coupling of the  $P_{13}(1720)$ , which might seem suprising as the helicity amplitudes from both works are very different. However, most of these differences cancel out in the isovector channel after proton- and neutron- amplitudes have been subtracted from each other (see Eq. 5). In the isoscalar sector this cancellation does not occur and both sets lead to very different predictions for  $f_{RN\omega}$ , see Sect. 4.

For the  $P_{13}(1720)$  and the  $F_{35}(1905)$  VMD is off by an order of magnitude. We argue that this mismatch does not hint on a failure of VMD, but has to be attributed to the unsatisfactory experimental information on these two resonances. Comparing the helicity amplitudes of the  $P_{13}(1720)$  obtained from different analyses [10, 15] reveals that neither their sign nor their magnitude are under control at all. Also the partial decay width into the  $\rho N$  channel is subject to large uncertainties, here the PDG and Manley differ by about a factor of three [10, 18, 19]. Obviously, the experimental



observation of this resonance is very complicated and its parameters might be sensitive to the details of the underlying theoretical model, such as the treatment of the non-resonant background. For a conclusive VMD analysis of these resonances it is therefore mandatory to enlarge the data base and to describe hadronic- and photoinduced reactions within one model. In [13] a VMD analysis for exactly these resonances was performed, leading to the general conclusion - in contradiction to this work - that VMD is not at all reliable in the resonance region.

Different parameterizations of the  $\rho$  decay width mainly influence the coupling constants of low-lying resonances. Since the PDG parameterization of the  $\rho$  decay (see Eq. 14) distributes more strength at invariant mass below the  $\rho$  meson pole mass, it leads to smaller values for the coupling constant, thus leading to an improved agreement between VMD and the hadronic fits. This effect is most notable for the  $D_{13}(1520)$  (see fourth and fifth column in Table 1).

Summarizing the results, we conclude that VMD can be applied in the resonance region on a phenomenological basis. We have shown that for the coupling constants  $f_{RN\rho}$  it leads to an approximate agreement with values adjusted to the hadronic decay width  $\Gamma_{RN\rho}$  with a tendency to somewhat underestimate these values. Therefore, our approach should yield reasonable predictions – at least for the lower limits – of the unknown coupling constants  $f_{RN\omega}$ .

## 4 Results for the $\omega$ : Strong Coupling of Sub-threshold Resonances

In this section we present our results for the coupling constants  $f_{RN\omega}$  following from the VMD analysis and discuss their compatibility with experimental information obtained from pion- and photon-induced  $\omega$ -production cross sections.

All nucleon resonances with  $j_R < \frac{7}{2}$ , for which helicity amplitudes have been extracted, are included. Thus we consider only one resonance above the  $N\omega$  threshold in our analysis, namely the  $D_{13}(2080)$ . Three different parameter sets for the helicity amplitudes are used, the results from the analysis of Arndt *et al* [9] and Feuster *et al* [15] as well as the values listed in the PDG [10]. The corresponding results for  $f_{RN\omega}$  together with the error-

bars are given in Table 2. We find a strong coupling to the  $N\omega$  channel in the  $S_{11}$ ,  $D_{13}$  and  $F_{15}$  partial waves; especially the  $S_{11}(1650)$ , the  $D_{13}(1520)$  and the  $F_{15}(1680)$  resonances show a sizeable coupling strength to this channel. In most cases the three parameter sets for the helicity amplitudes lead to similar results. As in the case of the  $\rho$  meson, however, for a few resonances ( $P_{11}(1440)$ ,  $S_{11}(1650)$  and  $P_{13}(1720)$ ) the differences are more pronounced. In particular, for the  $P_{13}(1720)$  the poor experimental situation does not allow a reliable extraction of the coupling strength, thus emphasizing the difficulties concerning this resonance which were already discussed in the previous section. The relatively large coupling constant for the  $D_{13}(1520)$  might at first seem surprising as the helicity amplitudes suggest that its electromagnetic decay is mainly an isovector one, corresponding to a small value for  $g_s$ . However,  $f_{RN\omega}$  is proportional to  $g_\omega$  (see Eq. 1), which is about three times larger than  $g_\rho$ . As a result, the  $\rho$  and  $\omega$  coupling are of the same size, but with a much larger error-bar for the  $\omega$  coupling.

It is noteworthy that the resonances with the largest coupling are well below the  $N\omega$  threshold. Subthreshold resonances in the  $N\omega$  channel are also reported elsewhere [8, 11]. In [8] it is shown that within a coupled-channel analysis the description of  $\pi N$  scattering enforces resonant structures in the  $N\omega$  channel. As in our work, strong contributions from the  $S_{11}$  and  $D_{13}$  partial waves are found. Quantitatively, both approaches yield quite different predictions for the coupling strength of the  $D_{13}(1520)$ , however. Whereas our VMD analysis predicts a coupling strength of about 3 (see Table 2), in [8] a value of  $f_{RN\omega} \approx 6.5$  is given. At the same time it is found in a quark model calculation [11] that the coupling constant of this resonance should be  $f_{RN\omega} \approx 2.6$ , which is surprisingly close to our result. However, from their quark model calculation the authors of [11] obtain initially coupling constants for hadronic Lagrangians which display very different energy dependences compared to ours. To be specific, in the case of the  $D_{13}(1520)$  close to threshold  $\omega$  and nucleon couple in a relative  $d$ -wave in their formalism, rather than forming an  $s$ -wave state as following from our Lagrangian, see Eq. 2 (which for example has also been employed in [8]). Thus a direct comparison of the results as done in [11] is possible only after simplifying assumptions, if at all.

A direct experimental observation of a resonant coupling of subthreshold resonances is very complex, since the resonances can add to the cross-sections only through the high-mass tails of their mass distribution and are therefore hard to disentangle from background effects. Sensitivity to the contribution

of subthreshold resonances in  $\omega$  production experiments can probably only be achieved by studying polarization observables. The current data do not permit such a project, however. As was pointed out in various previous works [20, 21, 22], an analysis of dilepton production on the nucleon in combination with VMD might provide further insight on this issue.

In spite of these difficulties, it is still rewarding to compare the VMD predictions with existing data on the reactions  $\pi^- p \rightarrow \omega n$  and  $\gamma p \rightarrow \omega p$ . Thus it is possible to infer if the predicted coupling constants of the subthreshold resonances produce a satisfactory overall agreement with data above the threshold. Comparison with data allows also to discuss the results for the  $D_{13}(2080)$ , the only resonance in our analysis above threshold. Based on recent data from photoproduction experiments, which display a richer structure than expected within a simple meson-exchange model, the search for resonances in the  $N\omega$  channel has so far concentrated on the mass range of approximately 1.8 – 2 GeV. At the current stage the data do not allow to pin down the quantum numbers of the involved resonances, however, and a variety of predictions exist [1, 2, 3, 4]. The  $D_{13}(2080)$  is not amongst them. In contrast to the photoproduction data, no experimental signature of a coupling of baryon resonances to the  $N\omega$  channel above the threshold has been detected in pion induced reactions [5]. We find for the  $D_{13}(2080)$  an  $\omega$  decay width of about 70 MeV and argue that its contribution to both reactions is too small to be seen in experiment.

As a first approximation, we take the full production amplitude as an incoherent sum of *Breit-Wigner* type amplitudes, describing  $s$ -channel contributions:

$$\sigma_{ab} = \sum_R \frac{2j_R + 1}{(2j_N + 1)\Omega_a} \frac{\pi}{k_a^2} \frac{\Gamma_a \Gamma_b}{(E_a - E_R)^2 + \Gamma_{tot}^2/4} \quad . \quad (15)$$

Here  $a$  stands for the incoming channel ( $\pi^- p$  or  $\gamma p$ ) and  $b$  for the  $\omega N$  channel.  $\Gamma_{a(b)}$  denote the respective partial decay width of the resonance and  $\Gamma_{tot}$  its total decay width, taking into account the  $\omega N$  decay as well. The energy dependence of the photon and the  $\omega$  decay amplitudes is obtained from the Lagrangians given in Eq. 2 and the formfactor of Eq. 9 with  $\Lambda = 1.0$ . Whenever possible,  $f_{RN\omega}$  is obtained from the helicity amplitudes from Arndt *et al*, otherwise the PDG estimates are used. For the remaining channels we take the parameterization from Manley *et al*. In Eq. 15  $\Omega_a$  is 1 for the pion and 2 for the photon.  $k_a$  is the cm-momentum of the particles in channel  $a$  and  $E_a$  denotes their cm-energy. All resonances listed in Table 2

are included. We stress that the only free parameter is the cutoff parameter  $\Lambda$ .

The results for both reactions are shown in Fig. 2 and Fig. 3. The data for the  $\pi$ -induced reaction are taken from [5] and we use the photoproduction data of [23]. The cross-section for  $\pi^- p \rightarrow \omega n$  is reproduced rather well, especially near threshold, whereas at high energies some strength is missing. This is in approximate agreement with the findings of the authors of [8], who are able to give a satisfactory description of this process around threshold in terms of subthreshold resonances. One can therefore conclude that the excitation of subthreshold resonances constitutes an essential ingredient to the production mechanism. This interpretation is confirmed by the fact that it is hard to understand this process in terms of non-resonant amplitudes only. Already the contribution from  $\rho_0$  exchange overestimates the data; only by suppressing the amplitudes by the introduction of very restrictive form factors a rough agreement with experimental data can be achieved [24]. Similar problems have been reported in [17] in a model that includes all Born terms. The contribution coming from the only resonance above threshold – the  $D_{13}(2080)$  – is about 0.1 mb, roughly 10% of the total cross-section. This is certainly too small to produce a distinguishable resonant structure in the total cross-section.

On the other hand, the photoproduction data can not be saturated within the resonance model. In particular, it seems futile to look for the  $D_{13}(2080)$  in this reaction. Since it is commonly assumed that the  $\pi^0$ -exchange as invoked in [25] plays a key role in the photoproduction we – incoherently – added this contribution using the same parameters as given in [25]. As shown in Fig. 3 the sum of both mechanisms yields a qualitative explanation of the data over the energy range under consideration.

It is not surprising that the resonance contribution is more likely to produce lower bounds for the cross-sections. We already discussed in Sect. 3, that the VMD analysis tends to underestimate the hadronic coupling constants. Also, at energies above the  $\omega N$  threshold, the helicity amplitudes of only a few resonances are known and the experimentally observed cross-sections have to be explained by additional production mechanisms, such as the  $\pi$ -exchange in the photoproduction. Keeping this in mind, the predictions of the resonance model are in reasonable agreement with the data and can be viewed as a confirmation of the VMD analysis.

## 5 The $\omega$ Meson in Nuclear Matter

In the previous section we discussed the relevance of resonances in the  $\omega N$  channel for an understanding of  $\omega$  production data. Here we study up to which extent the existence of these resonant states affects the properties of  $\omega$  mesons in nuclear matter. Of particular interest in this context is the fact that the VMD analysis predicts a strong coupling of subthreshold resonances, since in the case of the  $\rho$  meson it is widely acknowledged that its in-medium properties are dominated by low lying resonances, especially the  $D_{13}(1520)$ .

The in-medium properties of the  $\omega$  meson can be read off its spectral function, which is defined as:

$$A_{\omega}^{med}(\omega, \mathbf{q}) = \frac{1}{\pi} \frac{\text{Im } \Sigma_{tot}(\omega, \mathbf{q})}{(\omega^2 - \mathbf{q}^2 - m_{\omega}^2 - \text{Re } \Sigma_{med}(\omega, \mathbf{q}))^2 + \text{Im } \Sigma_{tot}(\omega, \mathbf{q})^2}. \quad (16)$$

Energy and three-momentum of the  $\omega$  meson are denoted by  $\omega$  and  $\mathbf{q}$ . The total self energy of the  $\omega$  meson  $\Sigma_{tot}$  is the sum of the vacuum and the in-medium self energies  $\Sigma_{vac}$  and  $\Sigma_{med}$ . In this work we neglect  $\text{Re } \Sigma_{vac}$  and approximate  $\text{Im } \Sigma_{vac}$  with the dominating  $3\pi$  decay width. We assume that this decay may only proceed via an intermediate  $\rho$  meson. The coupling constant  $f_{\omega\rho\pi}$  is adjusted to reproduce the vacuum decay width of 8.41 MeV [10].

To lowest order in the nuclear density  $\rho_N$ , the in-medium self energy of the  $\omega$  meson  $\Sigma_{med}$  in symmetric nuclear matter is given by:

$$\Sigma_{med} = \rho_N T_{\omega N}, \quad (17)$$

where  $T_{\omega N}$  is the spin/isospin averaged  $\omega N$  forward scattering amplitude. We approximate the scattering amplitude as a sum over all resonances which are discussed in this work and determine the resonance contributions in a non-relativistic approach.

For further details of the calculation the reader may consult our previous publication on the  $\rho$  meson [6, 7]. Both calculations are carried out within the same framework, differences appearing only in some minor points: First, the explicit values for the coupling constants and isospin factors are different. More crucial, we now evaluate the self energy in the cm-frame rather than in the rest frame of the nucleon. We do so since it has been demonstrated in [7] that thus a much better approximation of a relativistic calculation is achieved. As explained in [7], this leads in general to a reduction of the

results. Finally, at the  $\omega N R$  vertex the same formfactor is taken as in Eq. 9, in contrast to the choice in [6].

In Fig. 4 we show the spectral function for both an  $\omega$  meson at rest and moving with a momentum of 0.4 GeV with respect to the nuclear medium. The most obvious observation is that our model predicts an in-medium  $\omega$  meson which survives very well as a quasi-particle. At rest, its peak position is slightly shifted upwards by about 20 MeV, due to level-repulsion. The in-medium width is roughly 40 MeV as can be read off Fig. 5, where  $\Sigma_{med}$  is depicted for an  $\omega$  at rest. The  $\omega N$  forward scattering amplitude contains all elastic and inelastic channels. In the previous section we demonstrated that our model can give a good description of the important  $\pi N$  channel close to threshold. This enhances our belief that the VMD approach yields reasonable results for the in-medium properties of the  $\omega$  meson, especially for an  $\omega$  at rest.

By construction, the in-medium self energy develops resonant structures in the subthreshold region. The most important contributions come from the  $D_{13}(1520)$  and the  $S_{11}(1650)$  resonances. In contrast to the case of the  $\rho$  meson, these structures translate only into small bumps in the spectral function, reflecting - as follows from the coupling constants - that the  $\omega$  self energy is substantially smaller than that of the  $\rho$  meson.

Our value for the in-medium broadening of the  $\omega$  meson is in approximate agreement with that obtained in [17] and - in a dynamical simulation - in [26] and [27]. Also in the coupled channel analysis of [8] an in-medium broadening of 40 MeV for the  $\omega$  meson is reported. However, in this work the authors find that the  $\omega$  spectrum displays a richer structure in the subthreshold region, which is not surprising since their coupling constant for the  $D_{13}(1520)$  is much larger.

At higher momenta the influence of resonance-hole excitations gets reduced, see Fig. 4. Also, the longitudinal and transverse channel display a very similar behaviour (we therefore only show the results for the transverse channel). This is different from the case of the  $\rho$  meson, whose spectral function at large momenta receives a strong broadening in the transverse channel from the the coupling of  $p$ -wave resonances, for example the  $P_{13}(1720)$ , whilst the longitudinal mode is only slightly modified. In the case of the  $\omega$  meson however, only the  $F_{15}(1680)$  shows a sizeable coupling strength.

We have already mentioned that the  $\omega$  decay in vacuum proceeds mainly via an intermediate  $\rho$  meson. Due to kinematics, only the low-mass tail of the  $\rho$  mass spectrum is involved in this process. Consequently, if a lot

of  $\rho$  strength is shifted to smaller invariant masses in the nuclear medium – as is generally believed, see for example [6, 7, 28] – the  $\omega$  meson will receive additional broadening. We have estimated this effect by replacing the vacuum spectral function of the  $\rho$  with the in-medium one as given in [7] for the calculation of the  $\omega$  decay. To lowest order in the density, this corresponds to scattering processes like  $\omega N \rightarrow \pi R$ , where  $R$  stands for any baryon resonance included in the calculation in [7]; such processes have so far not been included in any calculation. We find an additional in-medium width for the  $\omega$  of about 40 MeV at the  $\omega$  mass from this process. It has to be pointed out, however, that we did not take into account the corresponding mass-shift of the  $\omega$  meson. Since the  $\omega$  decay width varies rapidly as a function of its mass, this is a strong simplification.

## 6 Summary

We have calculated the coupling strength of baryon resonances to vector mesons in a VMD approach. The isoscalar and isovector strength of the photon coupling are extracted by means of helicity amplitudes. For the isovector part we compare the VMD approach with fits to the hadronic decay width of the resonance into the  $N\rho$  channel. This allows to test the reliability of VMD in the resonance region. We find that VMD works well within a factor of two, with a tendency to underestimate the coupling strength.

In the  $\omega$  channel we find a strong coupling of subthreshold resonances, especially the  $D_{13}(1520)$  and the  $S_{11}(1650)$ . A direct experimental observation of these couplings is very complex and not possible within the current data base, which provides only an upper bound for the resonance contribution. We have calculated the total cross-section for the reactions  $\gamma N \rightarrow \omega N$  and  $\pi N \rightarrow \omega N$  with a simple *Breit-Wigner* ansatz and have shown that our coupling constants do not overestimate the data. In particular, the pion-induced reaction is very nicely described near threshold. We have argued that these results can be interpreted as a confirmation of the VMD model.

Guided by the observation, that the  $\rho$  meson properties in nuclear matter are strongly modified from the excitation of resonance-hole loops, we estimate these effects for the  $\omega$  meson. Since on average the  $\omega$  couples weaker to baryon resonances than the  $\rho$ , the effects are not as pronounced. In contrast to the  $\rho$  meson, the  $\omega$  survives very well as a quasi-particle. For an  $\omega$  at rest, we find an upward mass-shift of about 20 MeV and an in-medium broadening

of about 40 MeV. At higher momenta the medium modifications are further reduced. By taking into account also the possibility that in nuclear matter the  $\omega$  meson might decay into a modified  $\rho$  meson, we calculate an additional broadening of the  $\omega$  of about 40 MeV.

## 7 Acknowledgements

The authors gratefully acknowledge many stimulating discussions with V. Koch and the hospitality of the Nuclear Science Division of the LBNL, Berkeley, where parts of this work were completed. This stay was made possible through support by the NATO science program, NATO-collaborative research grant number 970102.

## References

- [1] V.D. Burkert, e-Print Archive: nucl-th/0005033.
- [2] Q. Zhao, H. Li, C. Bennhold, Phys. Rev. **C58** (1998) 2393.
- [3] Q. Zhao, H. Li, C. Bennhold, Phys. Lett. **B436** (1998) 42.
- [4] S. Capstick, W. Roberts, Phys. Rev. **D49** (1994) 4570.
- [5] A. Baldini *et al.*, in Landolt-Börnstein, vol 1/12 a (Springer, Berlin, 1987).
- [6] W. Peters, M. Post, H. Lenske, S. Leupold and U. Mosel, Nucl. Phys. **A632** (1998) 109.
- [7] M. Post, S. Leupold and U. Mosel, e-print Archive: nucl-th/0008027.
- [8] B. Friman, M. Lutz and G. Wolf, e-Print Archive: nucl-th/0003012 ; *Proceedings of the International Workshop XXVIII on Gross Properties of Nuclei and Nuclear Excitations: Hirschegg, Austria, 16-22 Jan 2000*, Editors: M. Buballa, B.-J. Schaefer, W. Nörenberg, J. Wambach.
- [9] R. A. Arndt *et al.*, Phys. Rev. **C52** (1995) 2120.
- [10] Particle Data Group, Eur. Phys. J. **C3** (1998) 1.



- [11] D. O. Riska and G. E. Brown, e-Print Archive: nucl-th/0005049.
- [12] H. B. O'Connell, B. C. Pearce, A. W. Thomas and A. G. Williams, Prog. Part. Nucl. Phys. **39** (1997) 201.
- [13] B. Friman and H.J. Pirner, Nucl. Phys. **A617** (1997) 496.
- [14] T. Ericson and W. Weise, *Pions and Nuclei*, Clarendon Press, Oxford, 1988.
- [15] T. Feuster and U. Mosel, Phys. Rev. **C59** (1999) 460.
- [16] T. Feuster and U. Mosel, Phys. Rev. **C58** (1998) 457.
- [17] F. Klingl, N. Kaiser and W. Weise, Nucl. Phys. **A624** (1997) 527.
- [18] D.M. Manley, R.A. Arndt, Y. Goradia and V.L. Teplitz, Phys. Rev. **D30** (1984) 904.
- [19] D.M. Manley and E.M. Saleski, Phys. Rev. **D45** (1992) 4002.
- [20] E.L. Bratkovskaya, O.V. Teryaev, V.D. Toneev, Phys. Lett. **B348** (1995) 283.
- [21] E.L. Bratkovskaya, M. Schäfer, W. Cassing, U. Mosel, O.V. Teryaev, V.D. Toneev, Phys. Lett. **B348** (1995) 325.
- [22] M. Soyeur, M. Lutz and B. Friman e-Print Archive: nucl-th/0003013 ; *Proceedings of the International Workshop XXVIII on Gross Properties of Nuclei and Nuclear Excitations: Hirschegg, Austria, 16-22 Jan 2000*, Editors: M. Buballa, B.-J. Schaefer, W. Nörenberg, J. Wambach.
- [23] ABBHHM-Colloboration, Phys. Rev. **75** (1968) 1669.
- [24] G.I. Lykasov, W. Cassing, A. Sibirtsev, M.V. Rzyanin, Eur. Phys. J. **A6** (1999) 71.
- [25] B. Friman and M. Soyeur, Nucl. Phys. **A600** (1996) 477.
- [26] T. Weidmann, E.L. Bratkovskaya, W. Cassing and U. Mosel, Phys. Rev. **C59** (1999) 919.

- [27] M. Effenberger, E.L. Bratkovskaya, W. Cassing and U. Mosel, Phys. Rev. **C60** (1999) 27601.
- [28] M. Urban, M. Buballa, R. Rapp and J. Wambach, Nucl. Phys. **A641** (1998) 433.

|                | $f_{RN\rho}(\text{Arndt})$ | $f_{RN\rho}(\text{Feuster})$ | $f_{RN\rho}(\text{PDG})$ | $f_{RN\rho}(\text{Man1})$ | $f_{RN\rho}(\text{Man2})$ | $f_{RN\rho}(\text{PDG})$ |
|----------------|----------------------------|------------------------------|--------------------------|---------------------------|---------------------------|--------------------------|
| $D_{13}(1520)$ | $3.44\pm0.18$              | 2.67                         | $3.42\pm0.20$            | $6.67\pm0.78$             | $5.79\pm0.68$             | $6.66\pm1.26$            |
| $S_{31}(1620)$ | $0.89\pm0.42$              | 0.10                         | $0.69\pm0.23$            | $2.14\pm0.30$             | $2.06\pm0.28$             | $2.61\pm1.01$            |
| $S_{11}(1650)$ | $0.70\pm0.08$              | 0.59                         | $0.57\pm0.31$            | $0.47\pm0.19$             | $0.45\pm0.18$             | $0.79\pm0.31$            |
| $F_{15}(1680)$ | $3.48\pm0.39$              | —                            | $3.14\pm0.37$            | $6.87\pm1.57$             | $6.36\pm1.45$             | $7.33\pm2.29$            |
| $D_{33}(1700)$ | $3.96\pm0.77$              | 3.68                         | $4.02\pm0.62$            | $1.96\pm0.67$             | $1.93\pm0.67$             | $4.91\pm1.57$            |
| $P_{13}(1720)$ | $0.25\pm0.42$              | 0.93                         | $0.19\pm0.79$            | $13.17\pm3.35$            | $12.09\pm3.17$            | $7.42\pm1.64$            |
| $F_{35}(1905)$ | $2.47\pm0.55$              | —                            | $2.56\pm0.75$            | $17.97\pm1.14$            | $17.57\pm1.12$            | $14.19\pm3.10$           |
| $P_{33}(1232)$ | $13.40\pm0.2$              | 11.96                        | $13.29\pm0.28$           | —                         | —                         | —                        |

Table 1: Listed are the hadronic coupling constants  $f_{RN\rho}$  obtained from the isovector electromagnetic amplitudes through a VMD analysis. The first column shows the results employing the helicity amplitudes from Arndt *et al* [9]. In the second column the helicity amplitudes from Feuster *et al* [15] are used instead and the third column shows the results obtained from the PDG estimates [10]. For comparison we show also the values for  $f_{RN\rho}$  resulting from direct fits to the partial decay width  $\Gamma_{RN\rho}$ . The values for  $\Gamma_{RN\rho}$  are taken from Manley *et al* [19] (4th column) and PDG (6th column), the  $\rho$  decay is parameterized according to Eq. 13. To point out further inherent uncertainties in the analysis, we show in the 5th column the results from a fit to Manley's values for the partial width, using the parameterization from Eq. 14 of the  $\rho$  spectral function.

|                | $\kappa$ | $f_{RN\omega}$ (Arndt) | $f_{RN\omega}$ (Feuster) | $f_{RN\omega}$ (PDG) |
|----------------|----------|------------------------|--------------------------|----------------------|
| $S_{11}(1535)$ | 4        | $1.27 \pm 1.58$        | 1.36                     | $0.76 \pm 1.23$      |
| $S_{11}(1650)$ | 4        | $1.59 \pm 0.29$        | 0.56                     | $1.12 \pm 1.09$      |
| $D_{13}(1520)$ | 8/3      | $2.87 \pm 0.76$        | 2.28                     | $3.42 \pm 0.87$      |
| $D_{13}(1700)$ | 8/3      | — — —                  | 1.88                     | $0.65 \pm 2.76$      |
| $D_{13}(2080)$ | 8/3      | — — —                  | — — —                    | $1.13 \pm 1.46$      |
| $P_{11}(1440)$ | 4        | $0.61 \pm 0.68$        | 1.26                     | $0.85 \pm 0.48$      |
| $P_{11}(1710)$ | 4        | $0.14 \pm 0.85$        | 0                        | $0.20 \pm 1.02$      |
| $P_{13}(1720)$ | 8/3      | $0.29 \pm 1.30$        | 2.18                     | $1.79 \pm 3.18$      |
| $F_{15}(1680)$ | 4/5      | $6.89 \pm 1.38$        | — — —                    | $6.52 \pm 1.49$      |

Table 2: The coupling constants  $f_{RN\omega}$  as extracted from the helicity amplitudes from the Arndt *et al* [9] (2nd column), Feuster *et al* [15] (3rd column) and the PDG group [10] (4th column). In the first column we give the values for  $\kappa$  (see Eq. 10).

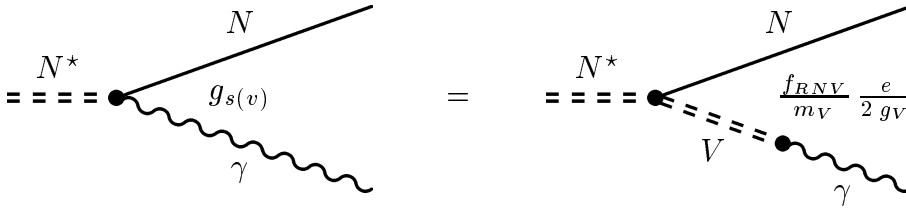


Figure 1: Diagrammatic description of the electromagnetic decay of a resonance in the VMD approach. The diagrams correspond to Eq. 1.

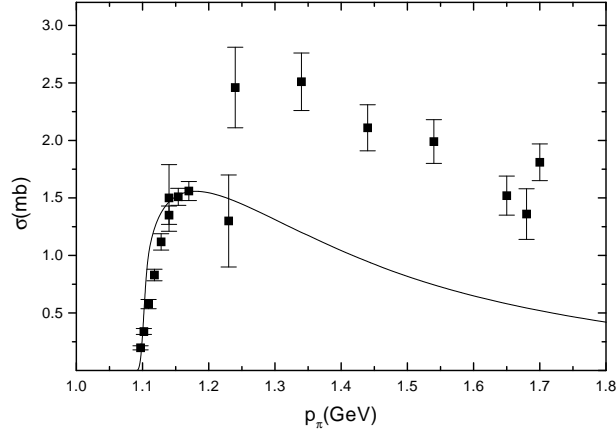


Figure 2: Total cross-section for the reaction  $\pi^- p \rightarrow \omega n$ . The data are taken from [5].

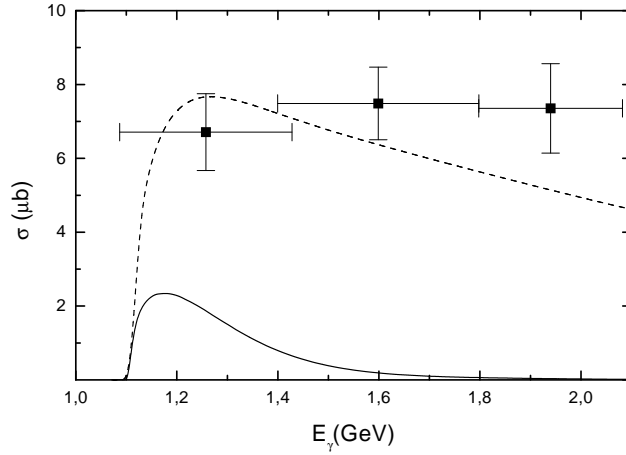


Figure 3: Total cross-section for the reaction  $\gamma p \rightarrow \omega p$ . The data are taken from [23]. The straight line shows the cross-section resulting from the resonance model, where the dashed line indicates the sum of resonance and pion-exchange contributions.

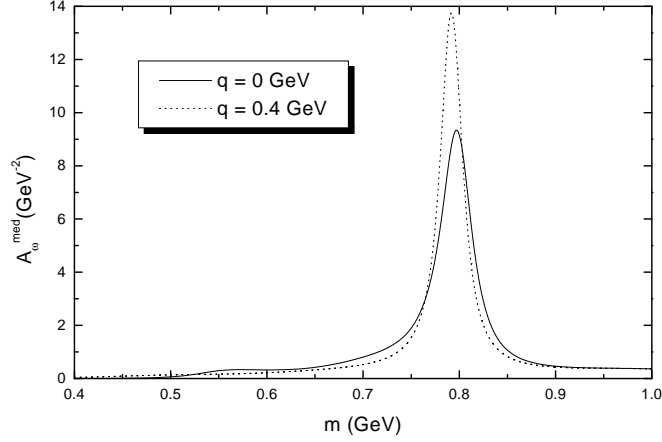


Figure 4: The spectral function of an  $\omega$  meson in nuclear matter versus its invariant mass  $m$ . Shown are results at  $q = 0$  GeV (solid line) and at  $q = 0.4$  GeV (dotted line). Only the transverse part is displayed. As discussed in the text, there is virtually no difference between transverse and longitudinal spectral function at 0.4 GeV.

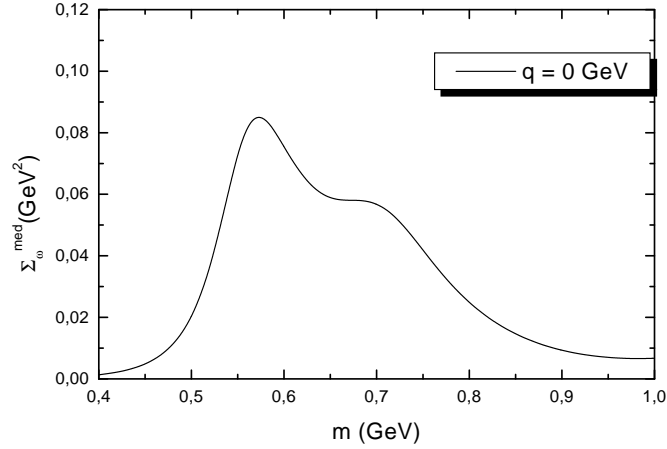


Figure 5: In-medium self energy of an  $\omega$  meson at rest as a function of its invariant mass  $m$ . One clearly sees resonant structures from the excitation of the  $D_{13}(1520)$  and the  $S_{11}(1650)$ .